Material Study of a Facade-Integrated Adsorption System for Solar Cooling of Buildings

Tim Dubies[1*], Olaf Böckmann[1], Micha Schäfer[1]

[1]*Institute for Building Energetics, Thermotechnology, and Energy Storage, University of Stuttgart, 70563 Stuttgart, Germany*
Correspondence author. Email: schaefer@igte.uni-stuttgart.de

ABSTRACT

Within the Collaborative Research Center 1244 at the University of Stuttgart, a facade-integrated solar cooling system for lightweight buildings is being developed. It addresses the reduction of CO2 emissions twofold. First, lightweight buildings require less concrete but require cooling due to their low thermal capacity. Secondly, the implementation of solar cooling systems counteracts the steadily growing global demand for energy for space cooling. The system is driven by a facade-integrated adsorber that has the functionality of an energy storage and is regenerated by absorbed solar irradiation. The desorbed water vapor is led into a condenser that is located on the opposite facade of the building. To provide cooling, the regenerated adsorber adsorbs water vapor from an evaporator located at the ceiling of the cooled room. The theoretical proof of concept was achieved in previous works, where a Matlab simulation model was developed. In this work, the influence of the adsorbent material on the system's behavior is investigated. Originally, zeolite 13X was considered and implemented into the model with the Dubinin-Asthakov approach. Here, the coefficients of the Dubinin-Asthakov equation are optimized for maximum cooling energy. For the identified range of beneficial values, coefficients of real working pairs are selected from the literature. In the results of this work, silica gels and modified zeolites, so-called zeotypes, show better performance, as they are suitable for lower desorption temperatures. The originally achieved cooling power with zeolite 13X was 1.15 kWh per day and can be increased to 1.47 kWh with the zeotype AQSOA-Z02 and 1.45 kWh with the silica gel RD2560. The resulting COP has improved from 0.243 to 0.311 and 0.308, respectively. Additionally, to the improved efficiency, the peak temperature of the adsorber is reduced.

Keywords: *Solar Energy, Thermal Energy Storage, Adsorption Chiller, Material Optimization, Building Energy Systems*

1. INTRODUCTION

The building sector is responsible for a huge share of total greenhouse gas emissions, as it accounts for 37% of the global CO_2 emissions [1]. The fastest-growing use of energy in buildings is space cooling. In [2], it is stated that it has tripled between 1990 and 2016 due to growing economies in hotter climates and general expectations for comfort in advanced economies. The share of energy usage in buildings for space cooling has reached 6% and is expected to grow.

To cut emissions from this growing energy demand, solar cooling stands out as a promising and renewable alternative to conventional cooling systems. A broad summary of different solar cooling technologies is given in [3]. A recent research project on solar cooling is currently being executed at the University of Stuttgart within the Collaborative Research Center 1244, where an exemplatory light-weight building is being constructed to be investigated for multiple research topics. One of those topics is an emission-free solar cooling system that is integrated into the facade of the building. The main driving force of the system is an adsorber that is regenerated by solar power. This paper will focus on the already established adsorption system as it investigates the effects of different adsorption working pairs in a given system setup.

The main motivation and related publications of the research project are listed in [4]. The goal of the project is to develop a solar cooling system for the thermal management of lightweight buildings. A detailed description of the planned solar cooling system is given in [5].

The system consists of three main components that are operated in two different main phases. An adsorber (A), a condenser (C) and an evaporator (E). In the first phase, the regeneration phase, the adsorber absorbs incoming solar radiation while gaining heat to desorb the uptaken water. The evaporated water vapor flows into the condenser, where it condenses and the resolving heat is ejected into the surrounding air. Therefore, the condenser

P. Droege and L. Quint (eds.), *Proceedings of the International Renewable Energy Storage and Systems Conference (IRES 2023)*, Atlantis Highlights in Engineering 32,
https://doi.org/10.2991/978-94-6463-455-6_16

is located on the shadowed side of the building. For the second phase, the adsorber will eventually be loaded again. Therefore, the condensate is pumped from the condenser into the evaporator, which is located on the ceiling of the cooled room inside the building. The desired cooling effect is achieved as the water evaporates in the evaporator while being adsorbed by the regenerated adsorber. Since it is not possible to operate both phases continuously, but it has to be switched between the cycles, the adsorber is regenerated in the morning while the cooling phase is activated in the afternoon. Currently, the system is designed for a working pair that has zeolite 13X as an adsorbate and water as a refrigerant.

Solar cooling systems are an intensively researched topic. There are multiple broad reviews of the current state of the art, such as [3], [6], [7]. One option for solar-powered cooling is the use of conventional compression cooling systems powered by photovoltaic cells. Other than that, there are multiple possibilities for solar-thermal cooling. They are categorized into open-loop systems using solid or liquid desiccants and closed-loop systems [6]. The closed-loop systems are mostly sorption systems, where absorption and adsorption systems are distinguished. In [3], insights on the temperature levels of these sorption systems are given. Desiccant and adsorption systems can provide cooling with heat sources under 100 °C. For higher temperature sources, absorption systems get more efficient. For the overall system design, this means that desiccant and adsorption systems can be combined with air collectors or flat plate collectors. Absorption systems are rather designed with concentrating solar collectors, such as linear fresnel or parabolic through collectors, reaching temperatures above 100 °C efficiently.

For the characterization of the different solar cooling systems, the temperature of the heat source as well as the possible temperatures of the cooled space are key parameters. Additionally, the coefficient of performance (COP) describes the overall efficiency of a system as the ratio of the achieved cooling energy to the incoming solar irradiation. When sorption processes are fueled by high temperatures, the COP is usually higher. In [6], the three levels of absorption systems are described that are called single-effect, double-effect, and triple-effect, respectively. A single-effect system can work with 85 °C as a heat source, achieving a COP of 0.7. A triple-effect adsorption system can use temperatures as high as 200 °C, yielding a COP of 1.7. For adsorption systems, which typically use significantly lower temperatures, the COP range is lower as well. In [6], COPs from 0.07 to 0.3 are achieved with adsorption systems.

Similar to this work, there are multiple papers that investigate different working pairs for adsorption processes. The most commonly used adsorbents with water as a refrigerant are zeolite and silica gel. Comparisons of these are made in [7], [3], [6], [8], [9], specifically for solar cooling devices. Some of them consider activated carbon as an adsorbent as well. However, activated carbon is mainly used with other refrigerants such as ammonia, methanol, or ethanol. In [6] a system using activated carbon and water is mentioned, yielding the lowest COP of 0.07. As another criteria for describing a certain system in the solar cooling domain, the desired temperature of the cooled environment has to be mentioned. A lot of publications focus on refrigeration besides cooling, such as [8], [6]. When temperatures reach 0 °C, the COPs go as low as 0.1.

The work of [3] focuses solely on air conditioning, where an example system using silica gel and water as a working pair yields a COP of 0.4-0.61. In [7], it is stated that both zeolite and silica gel are not beneficial for desired temperatures under 0 °C. Thereby, the adsorbents seem to be categorized as feasible working pair components for low source temperatures and moderate cooling temperatures, making them suitable for the air conditioning of buildings. On the other hand, a disadvantage of zeolites is their relatively high desorption temperature. Looking at the methodological aspects of simulation studies of adsorption systems, both [9] and [8] describe adsorption equilibria with the Dubinin-Astakhov-Equation (DAE).

Most of the named literature considers systems with conventional solar collectors, such as flat plate collectors or concentrating solar collectors. The facade integration of such systems seems to be underrepresented. However, in [10] there is a state-of-the-art review of the architectural integration of solar cooling systems in the facades of buildings. The paper considers sorption systems as a promising option. A system that is designed like the system in this work is not included.

In this work, the given system will be simulated with different adsorbents, while the refrigerant will remain the same. The goals are to improve the cooling power inside the building, lower the temperature in the adsorber, and use the mass of the adsorbent more efficiently. Therefore, the modeled characteristics of the working pairs will be altered, while other components, as well as their geometry and boundary conditions, will remain the same. Part of this work is a literature review of feasible adsorbents for solar cooling applications that can be implemented into the existing simulation model through the Dubinin-Astakhov (DA) approach.

In section 2 the fundamentals of adsorption that are relevant to the process are shown, as well as the selection of adsorbents considered in this study. The model equations that describe the behavior of the adsorber are presented, as well as the evaluation of performance for the alternation of adsorption materials. For the optimization of the working pair, section 3 shows a generic parameter study where the DAE coefficients are altered to get insights into the range of feasible coefficients. Based on these results, in section 4 the system is tested with promising working pairs from literature, to see which adsorbent leads to the most beneficial behavior of the system. Lastly, a conclusion of the achieved insights is drawn in section 5.

2. MODEL DESCRIPTION

In this chapter, the fundamentals of adsorption processes are described, as well as the materials that are commonly used as adsorbents. The description of the adsorption processes is focused on their modeling for the given system.

2.1. Fundamentals of Adsorption Processes

Adsorption can be described as a specific type of thermochemical energy storage where a reversible reaction is used to either charge or discharge energy from or to an external source. The reversible reaction in adsorption processes is the binding of a vapor or fluid onto the surface of a solid and, in the opposite direction, the release of vapor or fluid to the environment. The energy that is released during the adsorption is caused by Vander-Waals and electrostatic bounding forces between the adsorbed molecules and the adsorption material [11]. To be able to describe those processes more clearly, a common nomenclature is established, where the solid body is called the adsorbent. The vapor or fluid that is not bound to the surface of the adsorbent is called adsorptive, while the bound substance is called adsorbate. The adsorbate is mostly present in a fluid phase. A specific combination of an adsorbent and an adsorptive or adsorbate is called a working pair. Possible working pairs for solar cooling and their characteristics are described in [9]. Each working pair has a distinct behavior, regarding their process temperatures, pressures, and the energy that is either released or taken during the process. The exothermal reaction, where the adsorptive is bound onto the adsorbent as adsorbate, is called adsorption, while the reversed reaction is endothermal and called desorption. For the modeling of adsorption processes, three main characteristics have to be considered that vary for different working pairs:

- the reaction kinetics
- the equilibrium uptake
- the reaction enthalpy

In this study, the kinetics won't be considered, as the data for the described working pairs in literature rarely covers this component. Additionally, due to the slim geometry of the adsorbent and the slow reaction during the process, the kinetics are not the most relevant factor for the results. The simulated reactions are thereby following the equilibrium instantly.

2.1.1 Adsorption Equilibrium

The current uptake of a working pair can be described as

$$X = \frac{m_{\mathrm{adsorbate}}}{m_{\mathrm{adsorbent}}}. \tag{1}$$

The amount of adsorbate that is adsorbed is dependent on external factors such as temperature and pressure in the adsorber. However, there is a theoretical maximum uptake for a certain working pair. It is restricted by the surface area of the adsorbate and the characteristics of binding forces, etc. The maximum uptake is defined as X_0. Alternatively, the uptake can be expressed by the volume of the adsorbate relative to the mass of the adsorbent. In this case, W is commonly used as the volumetric uptake and W_0 as its possible maximum, respectively. To calculate the actual uptake in a given state, equilibrium models are used. In [12], a broad review of their use cases and characteristics is given. The equilibrium model that is used in this work is the DAE, where $X_{\mathrm{eq}} = f(T, p)$. The underlying theory holds that there is a force exerted on the adsorptive by the pores of the adsorbent. It is described as the adsorption potential A_{ad}, which is the energy that is needed to bring the adsorptive, from its current pressure p, into the saturation pressure p_{s}, as the adsorbate is present at saturation pressure [11]. The adsorption potential is calculated by the following equation:

$$A_{\mathrm{ad}} = R_{\mathrm{g}} T ln\left(\frac{p_{\mathrm{s}}}{p}\right), \tag{2}$$

where R_{g} is the ideal gas constant of the adsorptive and T is the current temperature.

With the adsorption potential A_{ad}, the DAE is expressed as

$$X_{\mathrm{eq}} = X_0\left[-\left(\frac{A_{\mathrm{ad}}}{E}\right)^n\right], \tag{3}$$

where the characteristic energy E is a measure for the adsorption forces between adsorbate and asorbent, while n describes the heterogeneity of the adsorbent's surface [12].

The DAE is a flexible method to describe the equilibria of adsorption working pairs in a fitting function. The parameters X_0, E, and n can be determined based on measurements of a given system or working pair.

Looking at the equation, the equilibrium uptake is increasing at higher pressure while decreasing when temperatures are high. Both pressure and temperature influence the adsorption potential A_{ad}, which is relative to E in the exponent in the DAE. Higher values for E result in a lower sensitivity of the equilibrium uptake to changes in either temperature or pressure. As stated before, E is the characteristic energy that is required for the adsorption process of a specific working pair. Thus, there is more temperature or pressure needed to accelerate adsorption processes in working pairs with higher values for E.

2.1.2 Adsorption Enthalpy

Finally, a crucial characteristic of the thermodynamics of adsorption processes is the released heat in the process. For a constant pressure, it can be described by the adsorption enthalpy. The adsorption enthalpy $\triangle H_{\mathrm{ads}}$ consists of the enthalpy of evaporation $\triangle H_{\mathrm{evap}}$ and the binding enthalpy $\triangle H_{\mathrm{b}}$. The latter $\triangle H_{\mathrm{b}}$ is decreasing

with an increasing uptake as the forces between adsorptive and adsorbent decrease. $\triangle H_{\mathrm{evap}}$, on the other hand, can be seen as constant for all degrees of uptake [11].

The rate of uptake X is described as

$$\theta = \frac{X}{X_0}. \tag{4}$$

If the adsorption equilibrium is described by the DAE in equation 3, the adsorption enthalpy can be expressed by the vant-Hoff equation:

$$-\triangle H_{\mathrm{ads}} = \triangle H_{\mathrm{evap}} + E\left(ln\frac{1}{\theta}\right)^{1/n} + \frac{E\beta T}{n}\left(ln\frac{1}{\theta}\right)^{-(n-1)/n}. \tag{5}$$

The parameter β is the thermal volumetric expansion coefficient of the adsorbate. The theory behind the equation is further described in [11] and [12].

Here again, E is a key coefficient in the equation. When E is high for a certain working pair, the adsorption enthalpy is high as well, leading to a higher energy demand for the actuation of the adsorption process.

2.2. Adsorbents

Adsorbents are porous solids that have a large surface area relative to their volume or mass. The bigger the surface area, the more adsorbate molecules can be adsorbed by the adsorbent, resulting in a higher capacity for the latter. However, it is explained in [12] that the desired behavior of adsorbents is only achieved if both the capacity and the kinetics of the adsorbent are high. While the surface area and capacity are strongly influenced by the micropore volume of the solid, fast kinetics require a network of macropores. Through those macropores, the adsorbate can diffuse easily, so that the micropore structures are reached. As a classification of pore sizes, pores with diameters below 2 nm count as micropores, while macropores have a diameter above 50 nm. The poresizes in between are called mesopores. Commonly used adsorbents are zeolite, silica gel, activated carbon, and activated carbon fiber. The characteristics of those will be briefly explained in the following. A more detailed explanation, regarding pore sizes and other technical characteristics, can be found in [12]. A summary of the chemical structure and basic elements of the adsorbents is given in [8]. The paper states that the named adsorbents are classified as physical adsorbents. Another class are chemical adsorbents, which mainly include metal chlorides, metal hydrides, and metal oxides. In [13], a recent publication is given where zeolite-like aluminum phosphates are examined regarding their performance for sorption refrigeration. The paper shows that newly synthesized adsorbents are a current research topic. However, this work is limited to the physical adsorbents named above.

2.2.1 Zeolite

Zeolite is an aluminasilicate crystal. Different types of zeolite appear naturally in sedimentary soils or can be synthesized artificially. The different types alter in their chemical composition, while they all consist of different proportions of aluminum, silicon, and oxygen ions [8]. In natural zeolites, there are cations such as Na, Ca, K, or Mg. 60 types of natural zeolites are known [14]. For refrigeration processes using adsorption, the natural zeolites chabazite, sodium chabazite, cowlesite, and faujasite come into use. For the artificial zeolites, there are about 150 types that get marked with letters, such as A, X, Y, or ZSM. For adsorption refrigeration, commonly used artificial zeolites are 4A, 5A, 10X, and 13X [8]. According to [12], artificial types are more widely used in technical applications as their characteristics can be specified better. Despite higher prices for synthetic zeolite, higher bulk densities and better heat transfer capabilities can be achieved compared to natural zeolites. The adsorption capacity of zeolite is dependent on the ratio between silicon and aluminum, while a lower ratio is beneficial for the adsorption ability. In comparison to the other adsorbents, the adsorption and desorption heat is considered high for zeolites, resulting in high desorption temperatures of about 250-300 °C [8].

2.2.2 Silica Gel

For the production of silica gel, a colloidal solution of silicic acid is coagulated [12]. The resulting porous solid consists of a framework of colloidal silica and hydrated SiO_4. The adsorption potential is achieved by the polar hydroxyl in the structure. It can form hydrogen bonds with polar oxydes, such as water and alcohol [8]. The amorphous form provides a network of interconnected pores and channels [15], resulting in a high internal surface area of 200 m²/g to 900 m²/g [12]. Silica gel is often used as a desiccant because of its hydrophilic behavior and large adsorption capacity. A unique characteristic is the relatively low regeneration temperature, as low as 150 °C [15].

2.2.3 Activated Carbon

Activated carbon is made of dried raw organic materials such as wood, coal, peat, bone, chark, coconut shells, or walnut hulls [16], [8]. Different methods are used to activate the materials, either physically or chemically. The physical activation process starts with carbonization (pyrolysis) in a neutral atmosphere, followed by the activation in oxydizing gases at high temperatures. For the chemical activation, the materials get treated with different chemicals at high temperatures. Physical activation is considered cheaper and better for the environment. However, the adsorption capacity of the resulting adsorbents is relatively low, while the heating process takes a lot of energy. Through chemical activation, the resulting adsorbents show a more porous structure and, therefore, a higher adsorption capacity.

On the other hand, the process takes longer, and toxic wastewater is produced [16].

The adsorption performance of activated carbon is influenced by functional groups that are connected to a structure of carboatomic rings. Arene groups increase adsorption, while sulfonic groups lower it. The functional groups on the surface of the activated carbon are affected by the organic precursor and the activation method. The surface area of activated carbon ranges from 500 to 1500 m²/g. In contrast to the other adsorbents, the surface of activated carbon is non-polar, resulting in a lower adsorption heat for working pairs with activated carbon. Another group of activated carbon that is distinguished by its fabrious structure is activated carbon fiber. It has a bigger surface area and better heat transfer performance than granular activated carbon. However, the thermal conductivity is dependent on the direction of the fibers. Additionally, the thermal resistance between the activated carbon fiber and the adsorber wall is higher [8].

2.3. Model Equations

The simulation model, on which this work is based on, is described in detail in [5]. The paper describes the model equations for the different elements of the system, as well as a simple switching heuristic as a control algorithm.

The dynamics of the adsorption process are defined relative to the mass of the adsorbent. It is mainly described by the uptake X, as a state, the working pair is currently in. The uptake of refrigerant a specific adsorbate can hold is a critical parameter for the working pair's behavior and is usually determined by experiments. The uptake is defined as the mass of refrigerant that is stored in the mass of adsorbent, as described by equation 1.

In the following, the equations describing the state of the adsorber are presented in both the cooling and regeneration modes.

2.3.1 Cooling Mode

In the cooling phase, the evaporator and adsorber are connected. The condenser is only exchanging heat with the environment. The exchanged water mass between the evaporator and condenser is described by the change in water uptake $\dot{X}_\mathrm{A}$ of the adsorption material. As adsorption kinetics are neglected, the change in uptake depends on the difference between the actual uptake of the adsorber X_A and the equilibrium uptake $X_\mathrm{eq}(T_\mathrm{A}, p_\mathrm{A})$. The latter is calculated by the DAE, shown in chapter 2.1.1 and depends on the current pressure p_A and temperature T_A in the adsorber. The following equations describe the state of the adsorber:

$$\dot{X}_\mathrm{A} = X_\mathrm{eq}(T_\mathrm{A}, p_\mathrm{A}) - X_\mathrm{A} \tag{6}$$

$$\dot{T}_\mathrm{A} = \frac{1}{m_\mathrm{ads}(c_\mathrm{ads} + X_\mathrm{A} c_\mathrm{w,ads}(T_\mathrm{A})) + m_\mathrm{m,A} c_\mathrm{m,A}} \Big(m_\mathrm{ads} \dot{X}_\mathrm{A} (\triangle H_\mathrm{ads}(T_\mathrm{A}) - R_\mathrm{s} T_\mathrm{A} + c_\mathrm{p,v}(T_\mathrm{E} - T_\mathrm{A})) + \dot{Q}_\mathrm{sol} - \dot{Q}_\mathrm{amb,A}(T_\mathrm{A}) \Big) \tag{7}$$

$$p_\mathrm{A} = p_\mathrm{E} = p_\mathrm{sat}(T_\mathrm{E}) \tag{8}$$

2.3.2 Regeneration Mode

In regeneration mode, the equations for the description of the adsorber are quite similar to those in cooling mode. The change in uptake is calculated by equation 6. This time, however, the uptake is declining because the equilibrium uptake $X_\mathrm{eq}(T_\mathrm{A}, p_\mathrm{A})$ is lower than the current uptake X_A due to the rising temperature T_A in the adsorber, leading to desorption.

The temperature change and pressure in the adsorber are calculated as follows:

$$\dot{T}_\mathrm{A} = \frac{1}{m_\mathrm{ads}(c_\mathrm{ads} + X_\mathrm{A} c_\mathrm{w,ads}(T_\mathrm{A})) + m_\mathrm{m,A} c_\mathrm{m,A}} \Big(m_\mathrm{ads} \dot{X}_\mathrm{A} (\triangle H_\mathrm{ads}(T_\mathrm{A}) - R_\mathrm{s} T_\mathrm{A}) + \dot{Q}_\mathrm{sol} \Big) \tag{9}$$

$$p_\mathrm{A} = p_\mathrm{C} = p_\mathrm{sat}(T_\mathrm{C}) \tag{10}$$

2.4. Evaluation of Performance

The measure for the performance of working pairs is the cooling power created by the system. It is calculated with the following equation:

$$\dot{Q}_\mathrm{cool} = \alpha_\mathrm{air}(T_\mathrm{R} - T_\mathrm{E}), \tag{11}$$

with α_air as the heat transfer coefficient between the evaporator and the surrounding air. T_R as the room temperature, constantly set to $23\,^\circ C$, and T_E as the temperature of the evaporator, calculated by the model equations. To get a comparable value for the working pairs, $\dot{Q}_\mathrm{cool}$ is integrated for one day to get the cooling energy Q_cool. As an indicator of performance, the COP is calculated by the following equation:

$$COP = \frac{Q_\mathrm{cool}}{Q_\mathrm{irr}}, \tag{12}$$

where Q_irr is the integral over one day of the incomming irradiation on the adsorbers surface area A_A:

$$\dot{Q}_\mathrm{irr} = A_\mathrm{A} \dot{q}_\mathrm{sol} \tag{13}$$

3. GENERIC PARAMETER STUDY

As described in the previous chapter, there are multiple parameters that have to be adjusted to simulate the behavior of different working pairs in the adsorber. As the adsoptive won't be changed in this study, the following parameters are varied to describe the behavior of the different adsorbents combined with water:

- characteristic Energy E $[\frac{\mathrm{J}}{\mathrm{kg}}]$
- Dubinin-Asthakov exponent n $[-]$
- maximum adsorption volume W_0 $[\frac{\mathrm{m}^3}{\mathrm{kg}}]$
- heat capacity of the adsorbent c_{ads} $[\frac{\mathrm{J}}{\mathrm{kgK}}]$
- true density of adsorbent ρ_{ads} $[\frac{\mathrm{m}^3}{\mathrm{kg}}]$
- void fraction of adsorbent ϕ $[-]$

The parameters that are used in this work are taken from literature giving values for them when the same DA approach is chosen and water is taken as an adsorptive. For different systems and experimental setups, the resulting values can be different, and the modeling method is only an approximation of the real adsorption dynamics. The consideration of multiple sets of values in this work should give an overview for the possible range of the different adsorbent materials. The results will show areas of possible values that can be beneficial for the system's performance. As stated before, the cooling energy Q_{cool} that is achieved during one run with a specific set-up is the indicator for that performance. In the following, the values found for the parameters are listed with their sources. For each material, the range of values for E, n, and W_0 are determined. The respective data for zeolite is shown in table 1, for silica gel in table 2, and for activated carbon in table 3.

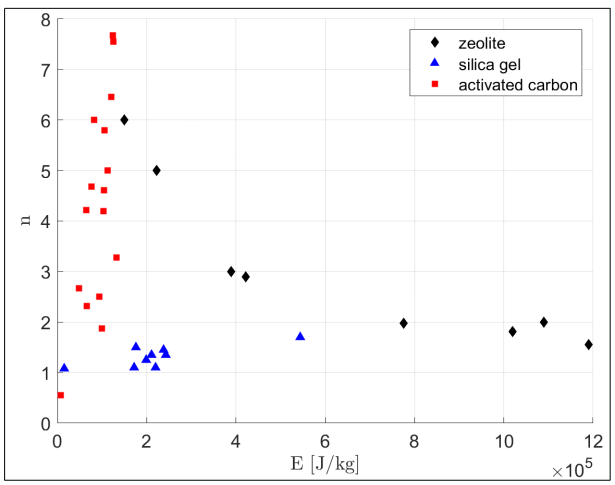

Figure 1 E and n values of DAE data found in literature

In a first generic parameter study, the system is simulated within the range of the found parameters. The goal is to see how the different DAE coefficients influence the behavior of a working pair and to find a possible optimum or beneficial range of DAE coefficients for the system. In the cited literature, where DAE coefficients are given, the heat capacity c_{ads}, true density ρ_{ads}, and void fraction ϕ are almost never given in addition. Therefore, those parameters are set to constant values for the parameter study. The chosen values are listed in table 4.

In terms of the environmental conditions, such as the solar radiation and the ambient temperature, a typical summer day in Stuttgart Vaihingen (Aug. 26th, 2016) is taken. In this location, an experimental setup of the system will be installed in the future. It is planned that the adsorber is oriented towards the south-east, corresponding to an azimuth angle of -45°. The slope of the adsorber surface area is considered 90°. The simulation time is 10 days for each run. The input data is the same for every day. Multiple days are simulated so that the system can swing into a steady cycling state. The results will show the respective values for the last day of the simulation time. The incoming solar radiation for one day is 4.72×10^3 Wh. This value is taken for the calculation of the COP according to equation 12.

The results are shown in a diagram, where the achieved cooling energy Q_{cool} is plotted over the characteristic energy E. In one plot, multiple results for different values of the exponent n are given. Each plot is thereby only accounting for one value of W_0.

The results for zeolite, with a W_0 of $1.3 \times 10^{-4} \frac{\mathrm{m}^3}{\mathrm{kg}}$, are shown in figure 2. The value for W_0 is the lower boundary of its possible range. The maximum cooling energy is between values for E of $2.4 - 4 \times 10^5 \frac{\mathrm{J}}{\mathrm{kg}}$, for all values of n considered. The curves with high values for n achieve higher cooling energies in the optimal areas for E and then decrease faster for higher values of E. The result looks similar for higher adsorption capacities W_0, although the maximum cooling energy is lower. With the upper boundary of $3.41 \times 10^{-4} \frac{\mathrm{m}^3}{\mathrm{kg}}$, the reached maximum is at 1400 Wh compared to the 1500 Wh with the result displayed. The optimal range of the characteristic energy E shifts slightly to higher values with an increasing adsorption capacity W_0. Another difference is the diminished slope of the curves until they reach their maximum and then shrink afterwards. When the specific values of zeolites listed in table 1 are compared with the diagrams, the most promising option is the zeotype AQSOA-Z02 from [19]. It is remarkable that all conventional zeolites have values for E that are greater than $10 \times 10^5 \frac{\mathrm{J}}{\mathrm{kg}}$. Those high values seem to be far away from the optimum.

The result for silica gel for a W_0 of $3.27 \times 10^{-4} \frac{\mathrm{m}^3}{\mathrm{kg}}$ is shown in figure 3. Here a similar picture is drawn as the maximum in cooling power is achieved with an E between $2 - 3 \times 10^5 \frac{\mathrm{J}}{\mathrm{kg}}$. Again, the maxima are slightly shifted towards higher values of E when higher values for W_0 are observed. Again, higher values for n seem to strike higher maximum values for the cooling energy. Contrary to the results of zeolites, the achieved cooling energy value increases with higher values for W_0. The maximum cooling energy is slightly above 1400 Wh. Thus, silica gels seem slightly worse than

Table 1. Dubinin-Astakhov Coefficients for zeolite/water working pairs

Adsorbent Name	$n\,[-]$	$E\left[\frac{J}{kg}\right]$	$W_0\left[\frac{m}{kg}\right]$	***Source***
Zeolite 13X	1.55	1.19×10^6	3.41×10^{-4}	[11]
Zeolite 13X	1.806	1.02×10^6	2.11×10^{-4}	[17]
Zeolite	2	1.09×10^6	2.69×10^{-4}	[18]
Zeotype: AQSOA-Z01	5	2.22×10^5	2.10×10^{-4}	[18]
Zeotype: AQSOA-Z02	3	3.89×10^5	3.10×10^{-4}	[19]
Zeotype: AQSOA-Z05	6	1.50×10^5	2.20×10^{-4}	[18]
Zeotype: ETS-10	1.98	7.76×10^5	1.29×10^{-4}	[18]
Min.	1.55	1.50×10^5	1.29×10^{-4}	
Max.	6	1.19×10^6	3.41×10^{-4}	

Table 2. Dubinin-Astakhov Coefficients for silica gel/water working pairs

Adsorbent Name	$n\,[-]$	$E\left[\frac{J}{kg}\right]$	$W_0\left[\frac{m}{kg}\right]$	***Source***
Silica Gel Alfonso	1.08	1.54×10^4	-	[20]
Silica Gel Wang	1.7	5.44×10^5	3.50×10^{-4}	[8]
Silica Gel Mohammed	1.45	2.38×10^5	-	[21]
A5BW	1.25	1.99×10^5	4.55×10^{-4}	[18]
RD2560	1.35	2.43×10^5	3.27×10^{-4}	[18]
Siogel	1.1	2.20×10^5	3.80×10^{-4}	[18]
Silica Gel Yang	1.1	1.72×10^5	5.92×10^{-4}	[18]
A++	1.35	2.11×10^5	4.89×10^{-4}	[18]
A++	1.5	1.76×10^5	4.71×10^{-4}	[22]
Min.	1.08	1.54×10^4	3.27×10^{-4}	
Max.	1.7	5.44×10^5	5.92×10^{-4}	

zeolites. However, these results are only theoretical, and it isn't yet confirmed that any of the real adsorbents in the literature could achieve these optimal values.

Looking at specific adsorbents in table 2, the RD2560 silica gel from [18] looks promising, as it yields the highest value for E below $5 \times 10^5 \frac{\mathrm{J}}{\mathrm{kg}}$. Another option, to be tested, is the silica gel of Wang [8], with a value for E of $5.4419 \times 10^5 \frac{\mathrm{J}}{\mathrm{kg}}$.

The results for activated carbon show no maximum. As the highest value for E is $1.33 \times 10^5 \frac{\mathrm{J}}{\mathrm{kg}}$ from MSC-V in [23], it is to be expected that all working pairs with activated carbons have too low characteristic energies to generate an optimal cooling power. For the comparison of specific working pairs, the former named MSC-V of [23] is considered.

4. SELECTED WORKING PAIRS

In the following, the most promising specific adsorbents that were identified in the parameter study in the previous section will be tested for the given solar cooling system. The results give a deeper insight into the system

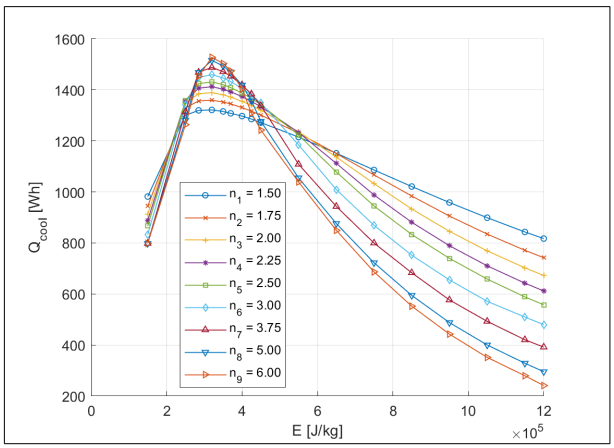

Figure 2 Cooling energy depending on DAE coefficients, Zeolite, $W_0 = 1.29 \times 10^{-4} \frac{m^3}{kg}$

Table 3. Dubinin-Astakhov Coefficients for activated carbon/water working pairs

Adsorbent Name	$n\,[-]$	$E\left[\frac{J}{kg}\right]$	$W_0\left[\frac{m}{kg}\right]$	***Source***
CMS	4.2	1.03×10^5	2.40×10^{-4}	[23]
U-03B	4.68	7.60×10^4	4.30×10^{-4}	[23]
U-03N	2.67	4.83×10^4	5.20×10^{-4}	[23]
U-02	2.32	6.61×10^4	4.50×10^{-4}	[23]
N-125	4.22	6.49×10^4	5.70×10^{-4}	[23]
DCG-5	1.87	9.94×10^4	4.90×10^{-4}	[23]
PLW	6.46	1.21×10^5	4.50×10^{-4}	[23]
PLWK	7.55	1.26×10^5	4.50×10^{-4}	[23]
ALCA	7.67	1.24×10^5	4.50×10^{-4}	[23]
MSC-V	3.28	1.33×10^5	1.70×10^{-4}	[23]
MSC-VR	4.61	1.05×10^5	1.70×10^{-4}	[23]
AC	0.55	7.11×10^3	-	[24]
CARBO-s	6	8.22×10^4	4.30×10^{-4}	[25]
MSC-V	5.8	1.06×10^5	4.00×10^{-4}	[25]
CMS	5	1.13×10^5	2.50×10^{-4}	[25]
DCG-5	2.5	9.38×10^4	5.40×10^{-4}	[25]
Min.	0.55	7.11×10^3	1.70×10^{-4}	
Max.	7.67	1.33×10^5	5.70×10^{-4}	

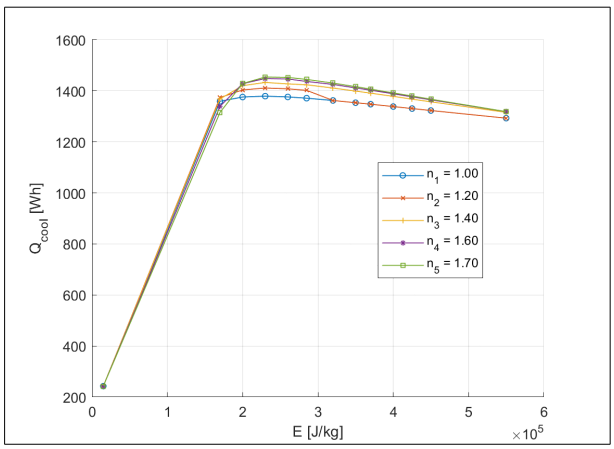

Figure 3 Cooling energy depending on DAE coefficients, Silica Gel, $W_0 = 3.27 \times 10^{-4} \frac{m^3}{kg}$

Table 4. Simulation properties of different adsorbents

Adsorbent Name	$\rho_{\text{ads}}\left[\frac{kg}{m^3}\right]$	$c_{\text{ads}}\left[\frac{J}{kgK}\right]$	$\phi\,[-]$
Zeolite	1150	880	0.4
Silica Gel	1400	975	0.5
Activated Carbon	2200	850	0.67

behavior for different working pairs, such as the current uptake X, the achieved evaporator temperature T_{E}, and the pressure p_{A}, as well as the temperature T_{A} in the adsorber. The coefficients for the selected adsorbents are shown again in table 5. In addition to the selected adsorbents, the originally used zeolite 13X is taken as a reference.

For all working pairs, the produced cooling energy is calculated, as is the COP of the system. To get a deeper insight into the processes, maximum and minimum values are given for the temperature of the adsorber T_{A}, the uptake of the adsorbent X, and the adsorption enthalpy h_{ads}. The minimum temperature of the evaporator T_{E} is given as well, while for all configurations, its maximum temperature is the room temperature of 23 °C. The results are dsiplayed in table 6.

The zeotype AQSAO-Z02 achieves the highest COP of 0.311 and a cooling energy of 1.47 kWh for one day. It is followed by the working pairs with silica gel, where RD2560 performs better with a COP of 0.308 and a cooling power of 1.45 kWh. The silica gel from

Table 5. Dubinin-Astakhov Coefficients for selected working pairs

Adsorbent Name	$n\,[-]$	$E\,\left[\frac{J}{kg}\right]$	$W_0\,\left[\frac{m^3}{kg}\right]$
Zeolite			
Zeolite 13X	1.55	1.19×10^6	3.41×10^{-4}
AQSOA-Z02	3	3.89×10^5	3.10×10^{-4}
Silica Gel			
RD 2560	1.35	2.43×10^5	3.27×10^{-4}
Silica Gel Wang	1.7	5.44×10^5	3.5×10^{-4}
Axtivated Carbon			
MSC-V	3.28	1.33×10^5	1.7×10^{-4}

Wang yields a COP of 0.290 with a cooling power of 1.37 kWh. The originally used zeolite 13X, with a COP of 0.243 and a cooling power of 1.15 kWh, is outperformed by all three former named working pairs. The tested working pair with the activated carbon MSC-V has a significantly lower COP than the other adsorbents, possibly confirming the supposition that working pairs with activated carbons and water are not suitable for solar cooling systems like the one tested in this work.

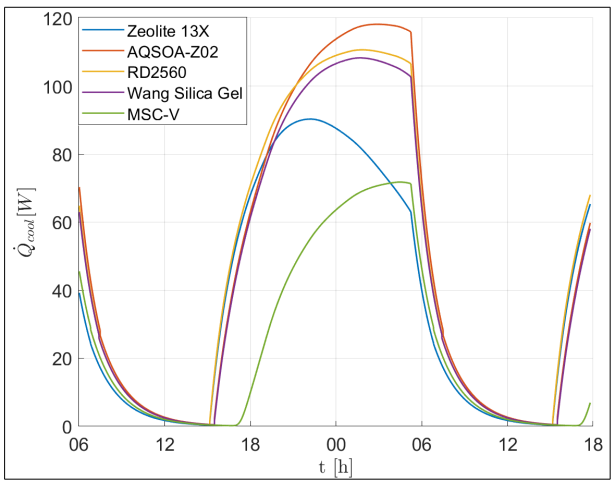

Figure 4 Cooling power over one day for selected working pairs

The respective trajectories of the cooling power $\dot{Q}_{\mathrm{cool}}$ for the selected adsorbents are displayed in figure 4. It is visible that the working pairs that achieve the lowest evaporator temperature yield the highest amplitude in cooling power. The zeotype AQSAO-Z02 yields the lowest evaporator temperature T_{E} with 6.1 °C, followed by RD2560 with 7.3 °C, and the silica gel of Wang with 7.5 °C. Additionally, the shapes of the cooling power varies, which can have consequences for comfort in the cooled room. The zeotype AQSOA-Z02 and the silica gels have relatively similar shapes. The cooling power is rising towards a maximum that is achieved towards the end of the cooling phase. The activated carbon follows a similar shape, while the cooling power itself is a lot smaller. In contrast, the cooling power of zeolite 13X stands out, as the peak is reached in the first half of the cooling phase. The power is then declining to reach around two-thirds of the maximum cooling power at the end of the cooling phase. The benefits of the shape of cooling power for comfort are not evaluated in this work. However, it is important to point out that the adsorption working pair can influence this behavior.

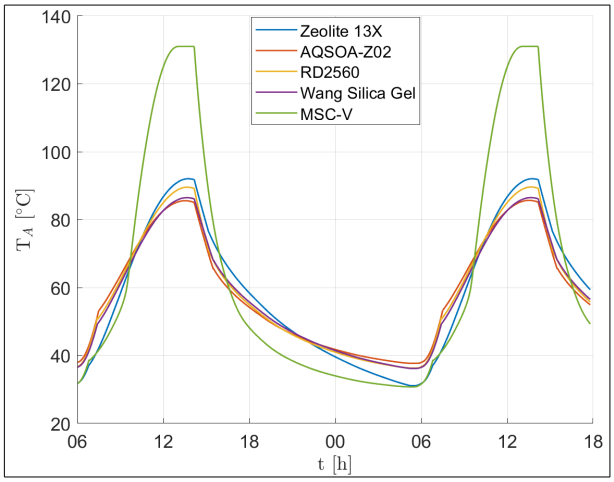

Figure 5 Adsorber temperatures for one day for selected working pairs

The temperatures of the adsorber T_{A} are shown in figure 5. The zeolites and silica gels have similar graphs, with differences in the extreme values. The biggest interval occurs with zeolite 13X and the lowest with the best-performing adsorbent AQSAO-Z02. Due to the higher uptake interval, the zeotype takes in more energy for desorption, resulting in a lower temperature in the regeneration phase. In the cooling phase, the adsorption energy is released, resulting in a higher minimum temperature. The smaller temperature deviation could be beneficial for the lifespan of components and side effects in the system. By far, the highest adsorber temperature is reached with the activated carbon.

The graphs of the uptake of the working pairs is shown in figure 5, for the same day as the previous diagrams. Except for MSC-V, all working pairs show a relatively similar trajectory of the uptake throughout the day. Looking at the numbers in table 6, it becomes clear that the better-performing working pairs yield an increased amplitude in uptake. While Zeolite 13X has a $\triangle X$ of $0.054\frac{\mathrm{kg}}{\mathrm{kg}}$, the change in uptake increases up to $0.07\frac{\mathrm{kg}}{\mathrm{kg}}$ with AQSAO-Z02. Another difference between the working pairs is the range in which this circulation is happening relative to the maximum uptake. As can be seen, zeolite 13X is circling in a relatively high range compared to the silica gel RD2560. The uptake of MSC-V is going as low as 0. The low value for E indicates that the desorption is done easily, but the adsorption doesn't work properly. The high adsorber temperatures occur during the regeneration phase, when the uptake X

Table 6. Results of simulations with specific working pairs

Adsorbent Name	Q_{cool} [kWh]	*COP*	T_{E} [°C]	$T_{\text{A,min}}$ [°C]	$T_{\text{A,max}}$ [°C]	$\triangle X$ $\left[\frac{\text{kg}}{\text{kg}}\right]$	$h_{\text{ads,min}}$ $\left[\frac{\text{kJ}}{\text{kg}}\right]$	$h_{\text{ads,max}}$ $\left[\frac{\text{kJ}}{\text{kg}}\right]$
Zeolite								
Zeolite 13X	1.15	0.243	10.2	31.1	92.0	0.054	2.98×10^6	2.75×10^6
AQSOA-Z02	1.47	0.311	6.1	37.8	85.4	0.070	2.80×10^6	2.73×10^6
Silica Gel								
RD2560	1.45	0.308	7.3	36.5	90.0	0.068	2.85×10^6	2.71×10^6
Silica Gel Wang	1.37	0.290	7.5	36.5	86.5	0.063	2.84×10^6	2.72×10^6
Activated Carbon								
MSC-V	0.76	0.160	12.9	31.3	131.0	0.034	3.22×10^6	2.60×10^6

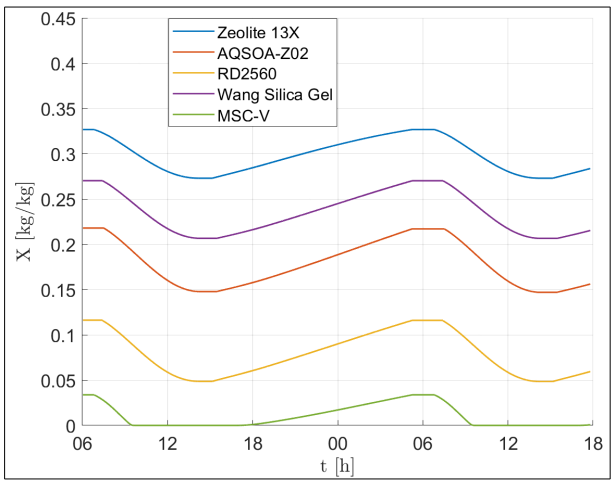

Figure 6 Current uptake X for selected working pairs

of MSC-V is 0. The reason for the high temperature is that there is no adsorbate to desorb at a certain point. Thereby, the incoming energy from irradiation is not deducted by the water vapor but is merely heating the thermal capacity of the adsorber mass.

5. CONCLUSION

In this work, a simulation model for a facade-integrated solar cooling system was used to identify beneficial adsorption working pairs for the system's behavior. For the modeling of the adsorption process, the Dubinin-Astakhov approach is used. Working pairs with water as a refrigerant were researched to get an overview of the possible range of DAE coefficients. In the first step, the most promising working pairs were selected through a parameter study. The study showed the optimal ranges for the three parameters in the DAE, where the characteristic energy E was identified as the most influential parameter on the performance of the system.

As a second step, a selection of specific working pairs containing zeolites, silica gels, and activated carbons were tested, and the results were compared to the originally used zeolite 13X. The performance of the system could be improved the most by the zeotype AQSOA-Z02, which is a modified zeolite for lower temperatures, and the silica gel RD2560. Additionally, silica gels in general seem more suitable for this specific system than conventional zeolites, which have high desorption temperatures. With the named adsorbents, the COP of the system could be boosted up to 0.311 from an original value of 0.243. Working pairs with activated carbon and water were identified as non-beneficial for the performance of the system. In addition, the use of the best-performing working pairs lowered the temperature range in the adsorber. The peak temperature in the adsorber got lowered by almost 7 °C to 85.4 °C. The results give insights on the trajectory of the cooling power curve throughout the day and the change in uptake for the tested working pairs.

While the results of this study confirm the expectations based on insights from the literature, the non-linear model showed numerical problems during the execution of simulations. Although those problems occurred mostly for working pairs that are probably not suitable for the given system, the accuracy of the results can be questioned. Additionally, estimations regarding the densities and heat capacities of the adsorbents were done, which can influence the results as well. For further investigations, a more detailed model of the adsorption process is in the making. Additionally, there is a physical testing system planned. The results of this study give insights into the possible working pairs and a direction for the search for an optimal configuration. However, the confirmation of the results has yet to be done by the more detailed model and, finally, the development of the system in reality.

ACKNOWLEDGEMENT

The authors thank the Deutsche Forschungsgemeinschaft (DFG, German Research Foundation) for funding under SFB1244-279064222.

REFERENCES

[1] UN environment programme, 2022 Global Status Report for Buildings and Construction: Towards a Zero-emission, Efficient and Resilient Buildings and Construction Sector, Nairobi, 2022.

[2] IEA - International Energy Agency, The future of cooling (2018).

[3] Q. Al-Yasiri, M. Szabó, M. Arıcı, A review on solar-powered cooling and air-conditioning systems for building applications, Energy Reports 8 (2022) 2888–2907. doi:10.1016/j.egyr.2022.01.172.

[4] University of Stuttgart, C06 - adaptive, facade-integrated adsorption systems for thermal management of lightweight buildings.

[5] J. L. Heidingsfeld, O. Böckmann, M. Böhm, O. Sawodny, Low order hybrid model for control design af an adsorption facade system for solar cooling (2022).

[6] I. Sarbu, C. Sebarchievici, Review of solar refrigeration and cooling systems, Energy and Buildings 67 (2013) 286–297. doi:10.1016/j.enbuild.2013.08.022.

[7] L. F. Cabeza, A. Solé, C. Barreneche, Review on sorption materials and technologies for heat pumps and thermal energy storage, Renewable Energy 110 (2017) 3–39. doi:10.1016/j.renene.2016.09.059.

[8] L. W. Wang, R. Z. Wang, R. G. Oliveira, A review on adsorption working pairs for refrigeration, Renewable and Sustainable Energy Reviews 13 (3) (2009) 518–534. doi:10.1016/j.rser.2007.12.002.

[9] A. Allouhi, T. Kousksou, A. Jamil, T. El Rhafiki, Y. Mourad, Y. Zeraouli, Optimal working pairs for solar adsorption cooling applications, Energy 79 (2015) 235–247. doi:10.1016/j.energy.2014.11.010.

[10] A. Prieto, U. Knaack, T. Auer, T. Klein, Solar coolfacades: Framework for the integration of solar cooling technologies in the building envelope, Energy 137 (2017) 353–368. doi:10.1016/j.energy.2017.04.141.

[11] B. Mette, Experimentelle und numerische untersuchungen zur reaktionsführung thermochemischer energiespeicher (2014).

[12] D. D. Do, Adsorption analysis: Equilibria and kinetics (1998).

[13] Z. Liu, J. Xu, M. Xu, C. Huang, R. Wang, T. Li, X. Huai, Ultralow-temperature-driven water-based sorption refrigeration enabled by low-cost zeolite-like porous aluminophosphate, Nature communications 13 (1) (2022) 193. doi:10.1038/s41467-021-27883-4.

[14] C. Colella, Natural zeolites and environment, in: Introduction to Zeolite Science and Practice, Vol. 168 of Studies in Surface Science and Catalysis, Elsevier, 2007, pp. 999–1035. doi:10.1016/S0167-2991(07)80815-9.

[15] P. Pourhakkak, A. Taghizadeh, M. Taghizadeh, M. Ghaedi, S. Haghdoust, Adsorption: Fundamental processes and applications, volume 33 - 1st edition: Chapter 2 - adsorbent (21.04.2023).

[16] Z. Heidarinejad, M. H. Dehghani, M. Heidari, G. Javedan, I. Ali, M. Sillanpää, Methods for preparation and activation of activated carbon: a review, Environmental Chemistry Letters 18 (2) (2020) 393–415. doi:10.1007/s10311-019-00955-0.

[17] K. Kowalska, B. Ambrożek, Modeling the performance of water-zeolite 13x adsorption heat pump, Archives of Thermodynamics 38 (4) (2017) 191–207. doi:10.1515/aoter-2017-0031.

[18] Z. Yang, K. R. Gluesenkamp, A. Frazzica, Equilibrium vapor pressure properties for absorbent and adsorbent materials (2020).

[19] S. Kayal, S. Baichuan, B. B. Saha, Adsorption characteristics of aqsoa zeolites and water for adsorption chillers, International Journal of Heat and Mass Transfer 92 (2016) 1120–1127. doi:10.1016/j.ijheatmasstransfer.2015.09.060.

[20] M. R. A. Afonso, V. Silveira Jr., Characterization of equilibrium conditions of adsorbed silica-gel/water bed according to dubinin-asthakov and freundlich (2005).

[21] R. H. Mohammed, O. Mesalhy, M. L. Elsayed, M. Su, L. C. Chow, Revisiting the adsorption equilibrium equations of silica-gel/water for adsorption cooling applications, International Journal of Refrigeration 86 (2018) 40–47. doi:10.1016/j.ijrefrig.2017.10.038.

[22] O. R. Fonseca Cevallos, Adsorption characterisitics of water and silica gel system for desalination cycle (2012).

[23] F. Stoeckli, T. Jakubov, Water adsorption in active carbons described by the dubinin-astakhov equation (1994).

[24] I. Solomon, Adsorption equilibrium of water vapor onto activated carbon, activated alumina, carbon and alumina impregnated with hygroscopic salt, TURKISH JOURNAL OF CHEMISTRY (2013). doi:10.3906/kim-1206-40.

[25] A. M. Slasli, M. Jorge, F. Stoeckli, N. A. Seaton, Water adsorption by activated carbons in relation to their microporous structure (2002).